
Regularized Training with Generated Datasets for Name-Only Transfer of Vision-Language Models

Minho Park Sunghyun Park Jooyeol Yun Jaegul Choo
Kim Jaechul Graduate School of AI, KAIST
{m.park, blizzard072, jchoo}@kaist.ac.kr
psh01087@gmail.com

Abstract

Recent advancements in text-to-image generation have inspired researchers to generate datasets tailored for perception models using generative models, which prove particularly valuable in scenarios where real-world data is limited. In this study, our goal is to address the challenges in fine-tuning vision-language models (*e.g.*, CLIP) on generated datasets. Specifically, we aim to fine-tune vision-language models to a specific classification model without access to any real images, also known as name-only transfer. However, despite the high fidelity of generated images, we observe a significant performance degradation when fine-tuning the model using the generated datasets due to the domain gap between real and generated images. To overcome the domain gap, we provide two regularization methods for training and post-training, respectively. First, as a post-training regularization, we leverage the domain-agnostic knowledge from the original pre-trained vision-language model via weight-space ensemble between the original model and the model fine-tuned on the generated dataset. Secondly, we reveal that fine-tuned models with high feature diversity score high performance in the real domain, which indicates that increasing feature diversity prevents learning the generated domain-specific knowledge. Thus, as a train-time regularization, we encourage feature diversity by providing additional regularization. Extensive experiments on various classification datasets and various text-to-image generation models demonstrate that our analysis and regularization techniques effectively mitigate the domain gap, which has long been overlooked, and enable us to achieve state-of-the-art performance by training with generated images. Code is available at <https://github.com/pmh9960/regft-for-gen>

1 Introduction

Recent advances in text-to-image generation have achieved remarkable success in producing high-quality images and capturing textual conditions [34, 39, 42–44]. In response to these developments, researchers have begun exploring ways to enhance the performance in perception tasks (*e.g.*, classification) by generating datasets from such powerful generative models [1, 2, 23, 45, 48, 49, 53]. Specifically, image-label pairs for classification can be constructed using pre-trained text-to-image generation models by conditioning the models to generate “A photo of a [class name]”. The generated datasets are particularly valuable when real-world samples are insufficient. In this study, we investigate the effective utilization of the generated datasets for fine-tuning vision-language models (*e.g.*, CLIP) in the name-only transfer scenario that solely relies on class names and does not have access to real images to classify images.

Despite the high fidelity of generated images, a notable domain gap persists between real and generated images. We quantify this gap using the Fréchet Inception Distance (FID) [25], which

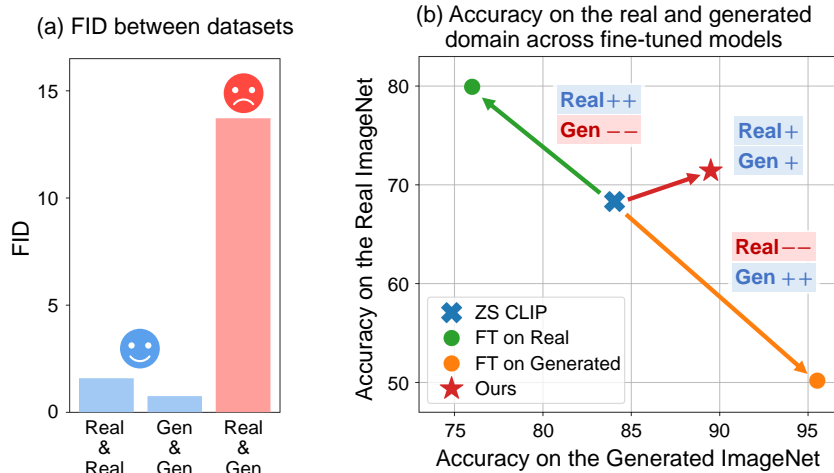


Figure 1: (a) Fréchet Inception Distance (FID) [25] of the intra-domain and inter-domain represents the significant domain gap between the real and generated images. (b) Accuracy of real and generated ImageNet [12] across the original pre-trained vision-language model (*e.g.*, CLIP [41]) and the fine-tuned models. Fine-tuning on the specific domain often leads to performance degradation of the other domain, as shown in both real and generated domains. In this study, we aim to improve the real-domain accuracy by overcoming the domain gap with regularization techniques.

assesses the disparity between image sets. As illustrated in Figure 1 (a), the gap between inter-domain (*e.g.*, Real-Gen) is significantly larger than the gap between intra-domain (*e.g.*, Real-Real, Gen-Gen). This domain gap leads to practical consequences when fine-tuning classifiers on the generated dataset. As shown in Figure 1 (b), fine-tuning classifiers on the specific dataset (*e.g.*, generated) can improve the in-domain accuracy (*e.g.*, generated), but often leads to performance degradation in the other domain (*e.g.*, real). Furthermore, since we observe that the accuracy of the generated dataset also degrades when fine-tuning it on the real dataset, *we interpret the situation as a subject of domain gap rather than the generated dataset’s inferiority or mislabeling.*

In this study, we introduce two regularization methods that are necessary to learn the task-specific information (*e.g.*, classification) from the generated dataset while overcoming the domain gap. The regularization methods can be applied at training and post-training, respectively. While previous name-only transfer approaches have refrained from fine-tuning the entire classifier and resorted to lightweight feature adapter [20, 23, 49, 53] or prompt engineering [33, 40], *we take the initiative to enhance the entire CLIP classifier including the image encoder* as illustrated in Figure 2.

First, to overcome the domain gap, we leverage the domain-agnostic knowledge from the original pre-trained vision-language model (*e.g.*, CLIP [41]) for regularizing fine-tuned models at the post-training time. We highlight that the simple ensemble approach can effectively learn additional task-specific knowledge from the generated dataset if we leverage the domain-agnostic knowledge from the original model, which is the most desirable property in the dataset generation literature.

Secondly, we introduce a training-time regularization to prevent learning the generated domain-specific knowledge when fine-tuning the classifier on the generated datasets. Based on a thorough analysis of fine-tuning with the generated dataset, we find that fine-tuned models with high feature diversity exhibit strong performance in the real domain. This suggests that increasing feature diversity can help prevent the model from learning domain-specific knowledge confined to the generated data. Therefore, we encourage feature diversity via training-time regularization loss.

Our extensive experiments showcase significant performance improvements across 11 name-only transfer datasets spanning various text-to-image generation models. Moreover, we further examine the wide applicability of our enhanced image encoder in the few-shot classification setting by simply replacing the original image encoder with ours, achieving state-of-the-art performance.

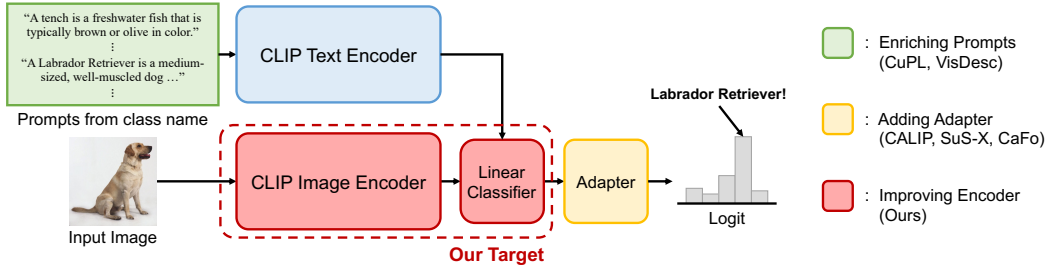


Figure 2: Overview of the architecture for name-only transfer of vision-language models (e.g., CLIP [41]). While the preceding approaches focused on **enriching prompts** (green) and **adapters** (yellow), we aim to **fine-tuning the CLIP image encoder** (red) with generated datasets.

2 Related Work

Name-only transfer of vision-language models In recent years, there has been a notable shift towards training vision foundation models by incorporating natural language supervision, as highlighted in several studies [26, 27, 38, 41]. Among these, CLIP [41] stands out for creating a joint embedding space for images and texts through contrastive learning, leveraging a vast dataset of 400 million image-text pairs. The name-only transfer is also pioneered by CLIP, which classifies images solely based on class names to assess similarity between images and texts. To achieve better performance than CLIP in the name-only transfer, enriching text input with large language models [5] has been researched [33, 40].

Dataset generation for name-only transfer More recently, there has been significant progress in constructing a generated dataset by harnessing pre-trained text-to-image models in the name-only transfer of vision-language models [23, 49, 53]. Specifically, these studies generated images from class names using textual input such as “A photo of a [class name]” to create the synthetic classification dataset. However, we reveal that fine-tuning the entire classifier with the generated dataset degrades the performance on the real dataset due to the domain gap as depicted in Figure 1.

To prevent the overfitting to the generated dataset, previous approaches often bypassed fine-tuning the CLIP image encoder and employed techniques such as linear probing [23] and adapters [49, 53], which are commonly used in few-shot classification scenario [17, 54]. Although the CLIP image encoder holds notable potential for enhancing classification performance, it remains relatively under-explored. In this paper, our target is the CLIP image encoder, which is the orthogonal research direction with the previous name-only transfer approaches as illustrated in Figure 2.

Fine-tuning CLIP with limited real datasets Besides the name-only transfer, training CLIP with an insufficient dataset has also been researched in various ways. CoOp [55], CLIP-Adapter [17], and Tip-Adapter [54] enhance the CLIP framework by freezing the image encoder and introducing small trainable modules. On the other hand, LPFT [30] introduces a two-step approach involving linear probing followed by full fine-tuning, while WiSE-FT [50] proposes a weight-space ensemble by blending weights between the zero-shot model and the fine-tuned model. Specifically, the weight-space ensemble has demonstrated significant efficacy in the natural distribution scenario (e.g., the photograph domain to the sketch domain). Notwithstanding these advancements, the impact of fine-tuning CLIP on a generated dataset remains unexplored. Thus, this study endeavors to examine the enhancements to CLIP through the incorporation of a generated dataset.

Representation Learning by Diversifying Features In the recent past, self-supervised learning has achieved huge success within the invariance learning framework [3, 6–9, 18, 19, 21, 36, 52]. Several studies emphasize the importance of increasing feature diversity in self-supervised learning and transfer learning, resulting in significant performance improvements in downstream tasks [3, 52, 56]. These approaches specifically aim to prevent informational collapse by reducing the off-diagonal elements of the covariance matrix over a batch while diversifying each element by enlarging the diagonal elements of the covariance matrix. Inspired by these pre-training approaches, we introduce two orthogonal metrics that assess the classifier’s change when fine-tuning on the generated datasets.

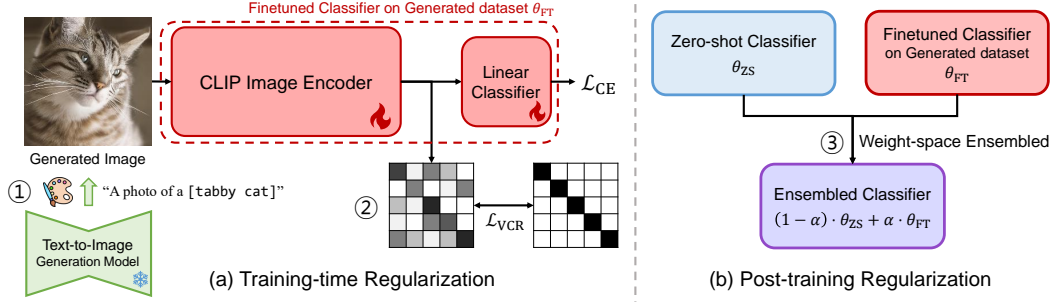


Figure 3: Overview of the proposed method. Initially, generated datasets are synthesized from textural conditions via text-to-image generation models. Subsequently, the entire classifier is fine-tuned on the generated dataset, employing cross-entropy loss (\mathcal{L}_{CE}) with variance-covariance regularization (\mathcal{L}_{VCR}). Lastly, a weight-space ensemble is performed to integrate the zero-shot classifier and the fine-tuned classifier.

3 Proposed Method

In this section, we provide our regularization methods based on our insight and analysis when fine-tuning the pre-trained vision-language model (*e.g.*, CLIP) on the generated datasets. The regularization methods are split into two parts: training-time and post-training regularization, as depicted in Figure 3.

3.1 Post-training Regularization: Weight-space Ensemble

As illustrated in Figure 1 (b), the real-domain accuracy degrades when fine-tuning on the generated dataset without any regularization. Importantly, we also emphasize that *the accuracy of the generated dataset also decreases when fine-tuning on the real dataset*, indicating that the performance degradation may be due to a domain gap rather than the inferiority or mislabeling of the generated dataset. Thus, we regularize the fine-tuned model with the generated dataset by leveraging the domain-agnostic property of the pre-trained vision-language model (*e.g.*, CLIP [41]).

Based on the interpretation, we conduct a weight-space ensemble [50] of the fine-tuned classifier with the zero-shot CLIP classifier as a simple yet effective post-training regularization to leverage the domain-agnostic property of the zero-shot CLIP, as depicted in Figure 3 (b). The weight-space ensemble is a simple linear interpolation between every parameter between two models (θ_{ZS}, θ_{FT}).

$$\text{WSE}(\theta_{ZS}, \theta_{FT}) = (1 - \alpha) \cdot \theta_{ZS} + \alpha \cdot \theta_{FT}, \quad (1)$$

where α is a weight mixing coefficient determining the ensemble ratio between the classifiers. The rationale behind this strategy is to leverage both the domain-agnostic property of the zero-shot CLIP classifier and the task-specific knowledge (*e.g.*, classification) of the fine-tuned classifier from the generated dataset. Although weight-space ensemble has originally been proposed to promote robustness in the natural distribution shift scenario, applying the technique to the models trained on generated datasets is under-explored. We bring attention to this technique by identifying our main obstacle in training with generated images as the domain gap, *a perspective that has been overlooked*.

By utilizing the domain-agnostic property of the zero-shot CLIP classifier, we can achieve task-specific knowledge from the generated datasets veiled by the domain gap between the real and generated images. Furthermore, due to its simplicity and flexibility, it can be applied in other perception applications (*e.g.*, detection, segmentation), which may suffer from the domain gap between the real and generated images to utilize the generated datasets.

3.2 How Does Fine-tuning on Generated Dataset Alter Classifiers?

In the following sections, we explore the correlation between feature diversity and performance experimentally, fine-tuning classifiers with various hyper-parameters on the generated dataset. Specifically, we examine the feature diversity of the classifiers using two orthogonal metrics: magnitude diversity (\mathcal{D}_{Mag}) and direction diversity (\mathcal{D}_{Dir}).

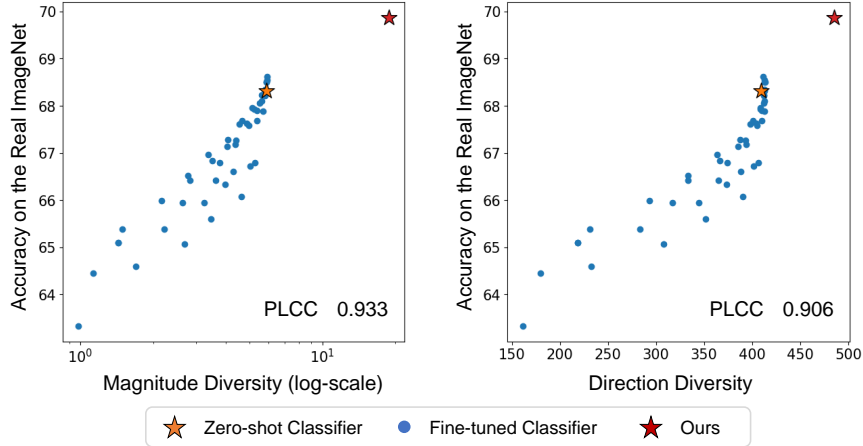


Figure 4: Evaluating magnitude diversity, direction diversity, and the real ImageNet [12] accuracy of fine-tuned classifiers with the generated dataset. The results indicate a strong correlation between the diversity and robustness of the real domain. According to the observation, we successfully improved the performance in the real domain via both regularization methods.

Magnitude Diversity (\mathcal{D}_{Mag}) Magnitude diversity pertains to the range of values for each feature element. We define the magnitude diversity of the classifier by utilizing a covariance matrix of the encoded features across dimensions. Particularly, the magnitude diversity is defined as the largest eigenvalue λ_{\max} of the covariance matrix, which represents the magnitude of the principal component. The following equations outline the calculation of the classifier’s magnitude diversity by extracting N test images into D -dimensional features (*i.e.*, $\mathbf{F} \in \mathbb{R}^{N \times D}$):

$$\text{Cov}(\mathbf{F}) = (\mathbf{F} - \mu_{\mathbf{F}})^T (\mathbf{F} - \mu_{\mathbf{F}}) \in \mathbb{R}^{D \times D}, \quad (2)$$

$$\mathcal{D}_{\text{Mag}} := \lambda_{\max}(\text{Cov}(\mathbf{F})), \quad (3)$$

where $\mu_{\mathbf{F}} \in \mathbb{R}^D$ denotes the mean vector of the rows of \mathbf{F} .

Direction Diversity (\mathcal{D}_{Dir}) Direction diversity concerns the variety of elements within the feature. Since it also expresses how orthogonal the features are, we leverage the covariance matrix again. We normalize the features with the square root of magnitude diversity ($\sqrt{\mathcal{D}_{\text{Mag}}}$) before calculating the covariance matrix to discard the influence of magnitude diversity (*i.e.*, set the magnitude diversity 1). Direction diversity is defined by taking the inverse of the L2 norm of the off-diagonal elements.

The rationale behind the definition of direction diversity is that a small off-diagonal element of the covariance matrix indicates a low similarity between two feature dimensions, and low similarities across all dimensions indicate high diversity. The following equations outline the calculation of the direction diversity from the same features:

$$\tilde{\mathbf{F}} := \frac{1}{\sqrt{\mathcal{D}_{\text{Mag}}}} \mathbf{F}, \quad (4)$$

$$\text{Cov}(\tilde{\mathbf{F}}) = (\tilde{\mathbf{F}} - \mu_{\tilde{\mathbf{F}}})^T (\tilde{\mathbf{F}} - \mu_{\tilde{\mathbf{F}}}) \in \mathbb{R}^{D \times D}, \quad (5)$$

$$\mathcal{D}_{\text{Dir}} := \frac{1}{\sqrt{\frac{1}{D(D-1)} \sum \sum_{i \neq j} (\text{Cov}(\tilde{\mathbf{F}})_{ij})^2}}, \quad (6)$$

where $\mu_{\tilde{\mathbf{F}}} \in \mathbb{R}^D$ denotes the mean vector of the rows of $\tilde{\mathbf{F}}$.

Analysis We assess the defined diversity of various fine-tuned models with the generated dataset.¹ The correlation between both diversity and the real accuracy is demonstrated in Figure 4, and it

¹We generate 64 images for 1000 ImageNet [12] classes by Stable Diffusion v2.1 [43] with “a photo of a [class name]” for generated training-set and generate additional 5000 images for extracting features with the fine-tuned classifiers. The hyper-parameter set is constructed by varying learning rate $\in \{3 \times 10^{-6}, 1 \times 10^{-7}, 3 \times 10^{-7}\}$, batch size $\in \{32, 64, 128\}$, and epochs $\in \{1, 2, 3, 5, 10\}$.

is also quantified by the Pearson linear correlation coefficient (PLCC) [16]. *We observed that the increasing performance on the real domain is highly related to the increasing feature diversity.* Thus, we introduce an additional regularization to increase the feature diversity of classifiers during fine-tuning classifiers on the generated datasets.

3.3 Training-time Regularization: Variance-Covariance Regularization

As illustrated in Figure 4, since classifiers that have high feature diversity often provide high real-domain accuracy, utilizing diversity metrics in training-time regularization is the straightforward approach to improve real-domain accuracy. However, both diversity metrics lack a closed-form derivative since the largest eigenvalue of the covariance matrix is computed by solving characteristic polynomials [28]. Thus, we have to discard the eigenvalue term from \mathcal{D}_{Mag} and \mathcal{D}_{Dir} while maintaining the main property of the metrics, resulting in the regularization techniques for the self-supervised learning, known as variance-covariance regularization [3, 56].

$$\mathcal{L}_{\text{VCR}} = \lambda_{\text{Var}} \cdot \frac{1}{D} \sum_{i=1}^D \max(0, 1 - \sqrt{C_{ii}}) + \lambda_{\text{Cov}} \cdot \frac{1}{D(D-1)} \sum_{i \neq j} C_{ij}^2, \quad (7)$$

where C is the covariance matrix over a mini-batch, D is the dimension of the embedding features, and $\lambda_{\text{Var}}, \lambda_{\text{Cov}}$ are the strength of the variance and covariance regularization, respectively.

Interpreting VCR in terms of $\mathcal{D}_{\text{Mag}}, \mathcal{D}_{\text{Dir}}$ The first term of the variance-covariance regularization increases the sum of the diagonal elements of the covariance matrix, which is equal to the sum of the eigenvalues [47]. Since increasing the largest eigenvalue can be circumvented by increasing the sum of all eigenvalues, increasing the magnitude diversity can be aimed by the first term. Furthermore, the second term reduces the off-diagonal elements of the covariance matrix, which can effectively increase the direction diversity. As a result, the variance-covariance regularization successfully increases both diversity and improves the real-domain performance as shown in Figure 4.

4 Experiments

4.1 Implementation Details

Our experiments are conducted across three text-to-image generation models: DALL-E [11, 42], Stable Diffusion 2.1 [43], and Stable Diffusion XL [39]. We generate 64 images per class, with a 5.0 guidance scale for achieving high-fidelity images. The input text prompts for text-to-image generation models for each dataset are demonstrated in Appendix G, which are given by previous name-only transfer research [23, 49, 53]. We employ CLIP ViT-B/16 [13, 41] as a pre-trained classifier. Additional implementation details for fine-tuning classifiers and the experiments for different visual backbones of CLIP, including ResNet-50 [22] were reported in Appendix A.

4.2 Name-only Transfer of Vision-Language Models

Datasets We carried out name-only transfer experiments across 11 datasets, covering a diverse range of objects, scenes, and fine-grained categories. These datasets include ImageNet [12], Caltech101 [15], DTD [10], EuroSAT [24], FGVC Aircraft [32], Flowers102 [35], Food101 [4], OxfordPets [37], StanfordCars [29], SUN397 [51], and UCF101 [46].

Experimental settings and baselines We compared our method with the following name-only transfer baselines. To begin with, we assess the zero-shot CLIP [41] with various textual templates, following the ensemble approach for text embeddings. CALIP [20] incorporates spatial information of the CLIP image features via parameter-free attention. CuPL [40], leveraging large-language models [5] to enrich prompts for CLIP text encoder, provides GPT prompts, so we evaluate classification performance using these given prompts. CaFo [53] initializes with the GPT prompts [5, 40] and fine-tunes the adapter using generated datasets. SuS-X [49], utilizing generated images as support set without additional fine-tuning, for a fair comparison, we use the provided generated datasets from DALL-E [42] by CaFo [53]. Since our proposed method can easily integrate with other name-only transfer approaches by replacing the CLIP image encoder, we adopt GPT prompts [5, 40] for the initial classifier and integrate with the adapter method [53].

Table 1: Comparison of accuracy on 11 name-only transfer benchmarks. Average indicates the average accuracy across the 11 datasets. Underline represents the highest accuracy achieved when utilizing generated datasets by DALL-E [42] given by CaFo [53], while **Bold** indicates the highest accuracy achieved without any constraints.

	Average	ImageNet [12]	Caltech101 [15]	DTD [10]	EuroSAT [24]	FGVC [32]
ZS CLIP	64.66	68.32	93.06	45.04	47.72	23.67
CALIP	64.92	68.68	93.91	44.98	47.51	23.43
CuPL	67.12	69.65	94.28	54.55	40.70	27.90
SuS-X (DALL-E)	68.14	70.19	93.43	54.49	<u>48.94</u>	27.81
CaFo (DALL-E)	68.22	70.63	<u>94.85</u>	54.96	48.56	28.47
Ours (DALL-E)	<u>69.31</u>	<u>70.87</u>	94.40	<u>56.68</u>	47.16	30.27
CaFo (SDv2.1)	67.46	70.20	94.52	54.73	39.36	28.02
CaFo (SDXL)	67.47	69.65	94.28	54.79	40.96	28.02
Ours (SDv2.1)	70.26	71.43	94.93	58.10	56.21	28.50
Ours (SDXL)	71.04	71.11	95.13	56.74	58.68	29.40
	Flowers102 [35]	Food101 [4]	OxfordPets [37]	StanfordCars [29]	SUN397 [51]	UCF101 [46]
ZS CLIP	66.10	83.85	87.11	66.29	65.13	65.00
CALIP	67.19	84.51	86.97	66.01	65.70	65.24
CuPL	69.47	86.35	90.54	66.62	68.00	70.29
SuS-X (DALL-E)	71.90	86.51	90.65	67.03	68.25	70.37
CaFo (DALL-E)	69.83	86.38	90.43	67.31	68.52	70.47
Ours (DALL-E)	73.28	86.53	<u>91.91</u>	<u>70.55</u>	<u>69.40</u>	<u>71.32</u>
CaFo (SDv2.1)	69.75	86.43	91.22	69.12	68.34	70.37
CaFo (SDXL)	69.79	86.35	90.87	69.21	68.00	70.29
Ours (SDv2.1)	71.30	86.41	92.40	72.74	69.88	70.98
Ours (SDXL)	72.76	86.35	92.50	78.40	68.84	71.50

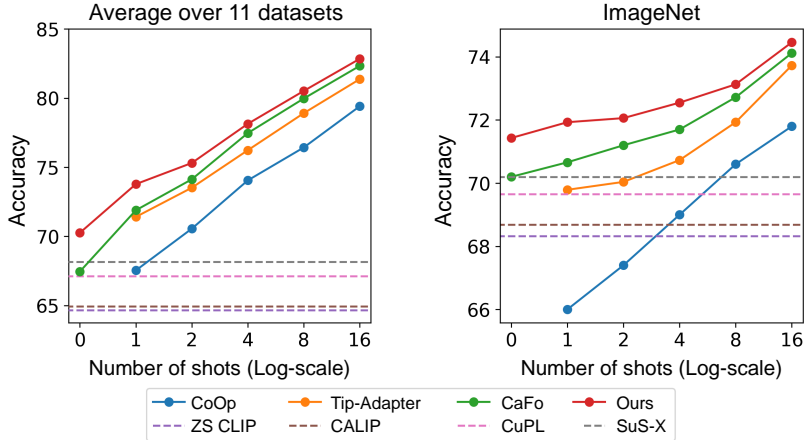


Figure 5: Comparison of accuracy in the few-shot classification. The left graph shows the average accuracy on 11 datasets, and the right graph indicates the accuracy on the ImageNet [12] dataset.

Main results Our extensive experiments demonstrate that our method significantly and generally outperforms the name-only transfer baselines in 11 datasets, as illustrated in Table 1. Our approach exhibited significant and general improvements on the DALL-E dataset, outperforming the zero-shot CLIP by +4.65 and the second-best approach, CaFo, by +1.11. These results indicate that we successfully regularize the fine-tuning CLIP classifier when using the generated datasets. Furthermore, as we extend the text-to-image generation model to SDv2.1 and SDXL, our method consistently outperforms across all datasets, whereas CaFo fails to show performance improvements with the change in generation models. More discussion of the effects of changing the text-to-image generation models is available in Appendix D. The compatibility of our method with the other name-only transfer approaches is discussed in Appendix F.

4.3 Few-shot Classification

Experimental settings and baselines We expand our approach to few-shot classification by upgrading the zero-shot CLIP classifier to our enhanced classifier, which was fine-tuned on the

Table 2: Ablation studies of the fine-tune classifier, weight-space ensemble and variance-covariance regularization on 11 datasets.

Fine-tune Classifier	Weight-space Ensemble	\mathcal{L}_{VCR}	Average Accuracy
✗	✗	✗	67.12
✓	✗	✗	53.79
✓	✓	✗	69.13
✓	✓	✓	69.56



Figure 6: Real ImageNet [12] accuracy according to the scale of generated datasets.

Table 3: Finding the mixing coefficient α for mixing between zero-shot CLIP and fine-tuned CLIP on the generated ImageNet dataset.

α	0.0	0.1	0.2	0.3	0.4	...	1.0
ImageNet Accuracy	68.32	69.78	69.73	68.69	67.08	...	48.31
+ Improvement	-	+1.46	+1.41	+0.37	-1.24	...	-20.01

generated dataset for name-only transfer. The generated datasets are given by Stable Diffusion 2.1 [43] across all approaches that utilize generated datasets. The models are trained with 1, 2, 4, 8, and 16 shots for each dataset and evaluated using the full test sets following the few-shot classification experiments [54]. We compare the performance with other CLIP-based adaptation approaches, which include CoOp [55], Tip-Adapter [54], and CaFo [53].

Main results As shown in Figure 5, our fine-tuned classifier consistently outperforms the baselines in the few-shot classification. Since our proposed method aimed to utilize the generated dataset in the scenario that does not have access to real images, the performance improvements decreased with the number of real images. Nevertheless, our approach still demonstrates superior performance compared to few-shot baselines. These results indicate that enhancing the CLIP image encoder using our method is also effective in data-scarce scenarios by integrating with other few-shot classification approaches. The detailed experiments for all datasets are available in Appendix C.

4.4 Analysis

Ablation study The ablation study of the proposed method is conducted across all 11 datasets in the name-only transfer. We utilize generated datasets from Stable Diffusion 2.1 [43], and we do not utilize the adapter [53] due to clearly showing the ablation study. As depicted in Table 2, our investigation reveals that the weight-space ensemble performs exceptionally well in overcoming the domain gap between real and generated images. Although the fine-tuned CLIP model on the generated dataset showed significant degradation in real-world performance, the weight-space ensemble demonstrated its effectiveness by combining the zero-shot CLIP’s domain-agnostic knowledge with the fine-tuned CLIP’s task-specific expertise. Furthermore, the variance-covariance regularization (\mathcal{L}_{VCR}) also showed additional improvements. The additional improvements support our analysis of feature diversity, which shows that high diversity can help improve performance in the real domain. While the improvement from variance-covariance regularization is not substantial compared to the weight-space ensemble, both regularization methods demonstrated consistent improvements across all datasets, as shown in Appendix B.

Number of generated samples We conducted an analysis of the performance improvement based on the scale of the generated dataset given by Stable Diffusion 2.1 [43] on the ImageNet [12] dataset. As illustrated in Figure 6, the performance on the real domain increased according to the scale of the generated datasets. While previous name-only transfer approaches [49, 53] only utilized 2 generated images per class, our performance still increased by 256 images per class. Due to our limited resources, we have ceased experimenting with more than 256 images per class. Nevertheless,

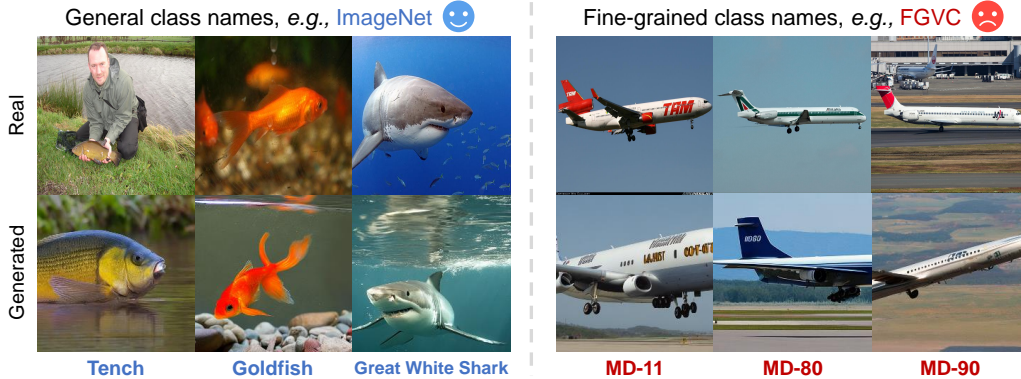


Figure 7: Although Stable Diffusion effectively synthesizes general images owing to its proficiency in handling general class names (*e.g.*, ImageNet [12]), it encounters challenges in generating images within specific domains from fine-grained class names (*e.g.*, FGVC Aircraft [32]).

there is a potential for further scaling beyond this threshold, which could be explored using scaling laws similar to those discussed in a recent study [14].

Finding the mixing coefficient Determining the weight mixing coefficient is a crucial feature of the proposed method. Unlike other hyper-parameters, such as the learning rate or the number of epochs, which require searching during training, the mixing coefficient can be effectively identified by evaluating the validation set post-training. In our experiments, the mixing coefficient is explored in intervals of 0.1 from 0 to 1. The accuracy on the ImageNet [12] test set corresponding to the mixing coefficient α is presented in Table 3. Despite using a grid search with a relatively large interval for the mixing coefficient, it successfully integrates the zero-shot classifier and the fine-tuned classifier, demonstrating substantial performance improvements and highlighting the effectiveness of our approach. The specific mixing coefficients for each dataset, adjusted according to the domain gap between the real and generated datasets, are available in Appendix E.

5 Limitations and Discussion

Although the proposed approach is the first to tackle the domain gap between real and generated images, our performance is dependent on the capability of the generative model to synthesize various subjects. As depicted in Figure 7, generated images from general class names, such as ImageNet [12], exhibit high fidelity and accurately represent the target class name. However, for narrow domains beyond the capability of Stable Diffusion, such as the FGVC [32], the generated samples do not contain sufficient task-specific content. Despite the huge success of text-to-image generation, addressing the challenges of generating images for specific domains remains a crucial avenue for future research.

6 Conclusion

In this paper, we demonstrate the importance of addressing the domain gap between real and generated images, highlighting it as a crucial factor of performance degradation when fine-tuning exclusively with generated data. Specifically, our in-depth analysis reveals that the primary obstacle for using generated images is not the quality of generated images (*e.g.*, mislabeled samples), but rather the domain gap between real and generated samples. Through our train-time and post-training regularization techniques for mitigating the domain gap, we are able to improve the image encoder itself, without using additional parameters such as adapters.

Additionally, our findings can be seamlessly integrated into few-shot learning scenarios, also achieving state-of-the-art performance. While our primary experiments have focused on classification, our approach is highly adaptable to scenarios where generated images can supplement existing datasets (*e.g.*, detection, segmentation), which we consider as promising future work.

References

- [1] Shekoofeh Azizi, Simon Kornblith, Chitwan Saharia, Mohammad Norouzi, and David J Fleet. Synthetic data from diffusion models improves imagenet classification. *arXiv preprint arXiv:2304.08466*, 2023.
- [2] Hritik Bansal and Aditya Grover. Leaving reality to imagination: Robust classification via generated datasets. *arXiv preprint arXiv:2302.02503*, 2023.
- [3] Adrien Bardes, Jean Ponce, and Yann LeCun. Vicreg: Variance-invariance-covariance regularization for self-supervised learning. In *International Conference on Learning Representations*, 2022.
- [4] Lukas Bossard, Matthieu Guillaumin, and Luc Van Gool. Food-101—mining discriminative components with random forests. In *Computer Vision—ECCV 2014: 13th European Conference, Zurich, Switzerland, September 6–12, 2014, Proceedings, Part VI 13*, pages 446–461. Springer, 2014.
- [5] Tom Brown, Benjamin Mann, Nick Ryder, Melanie Subbiah, Jared D Kaplan, Prafulla Dhariwal, Arvind Neelakantan, Pranav Shyam, Girish Sastry, Amanda Askell, et al. Language models are few-shot learners. *Advances in neural information processing systems*, 33:1877–1901, 2020.
- [6] Mathilde Caron, Ishan Misra, Julien Mairal, Priya Goyal, Piotr Bojanowski, and Armand Joulin. Unsupervised learning of visual features by contrasting cluster assignments. *Advances in neural information processing systems*, 33:9912–9924, 2020.
- [7] Mathilde Caron, Hugo Touvron, Ishan Misra, Hervé Jégou, Julien Mairal, Piotr Bojanowski, and Armand Joulin. Emerging properties in self-supervised vision transformers. In *Proceedings of the IEEE/CVF international conference on computer vision*, pages 9650–9660, 2021.
- [8] Ting Chen, Simon Kornblith, Mohammad Norouzi, and Geoffrey Hinton. A simple framework for contrastive learning of visual representations. In *International conference on machine learning*, pages 1597–1607. PMLR, 2020.
- [9] Xinlei Chen and Kaiming He. Exploring simple siamese representation learning. In *Proceedings of the IEEE/CVF conference on computer vision and pattern recognition*, pages 15750–15758, 2021.
- [10] Mircea Cimpoi, Subhansu Maji, Iasonas Kokkinos, Sammy Mohamed, and Andrea Vedaldi. Describing textures in the wild. In *Proceedings of the IEEE conference on computer vision and pattern recognition*, pages 3606–3613, 2014.
- [11] Boris Dayma, Suraj Patil, Pedro Cuenca, Khalid Saifullah, Tanishq Abraham, Phuc Le Khac, Luke Melas, and Ritobrata Ghosh. Dall · e mini, 7 2021.
- [12] Jia Deng, Wei Dong, Richard Socher, Li-Jia Li, Kai Li, and Li Fei-Fei. Imagenet: A large-scale hierarchical image database. In *2009 IEEE conference on computer vision and pattern recognition*, pages 248–255. Ieee, 2009.
- [13] Alexey Dosovitskiy, Lucas Beyer, Alexander Kolesnikov, Dirk Weissenborn, Xiaohua Zhai, Thomas Unterthiner, Mostafa Dehghani, Matthias Minderer, Georg Heigold, Sylvain Gelly, et al. An image is worth 16x16 words: Transformers for image recognition at scale. In *International Conference on Learning Representations*, 2021.
- [14] Lijie Fan, Kaifeng Chen, Dilip Krishnan, Dina Katabi, Phillip Isola, and Yonglong Tian. Scaling laws of synthetic images for model training... for now. *arXiv preprint arXiv:2312.04567*, 2023.
- [15] Li Fei-Fei, Rob Fergus, and Pietro Perona. Learning generative visual models from few training examples: An incremental bayesian approach tested on 101 object categories. In *2004 conference on computer vision and pattern recognition workshop*, pages 178–178. IEEE, 2004.
- [16] David Freedman, Robert Pisani, and Roger Purves. Statistics (international student edition). *Pisani, R. Purves, 4th edn. WW Norton & Company, New York*, 2007.
- [17] Peng Gao, Shijie Geng, Renrui Zhang, Teli Ma, Rongyao Fang, Yongfeng Zhang, Hongsheng Li, and Yu Qiao. Clip-adapter: Better vision-language models with feature adapters. *International Journal of Computer Vision*, pages 1–15, 2023.
- [18] Quentin Garrido, Yubei Chen, Adrien Bardes, Laurent Najman, and Yann LeCun. On the duality between contrastive and non-contrastive self-supervised learning. In *The Eleventh International Conference on Learning Representations*, 2023.

- [19] Jean-Bastien Grill, Florian Strub, Florent Alché, Corentin Tallec, Pierre Richemond, Elena Buchatskaya, Carl Doersch, Bernardo Avila Pires, Zhaohan Guo, Mohammad Gheshlaghi Azar, et al. Bootstrap your own latent—a new approach to self-supervised learning. *Advances in neural information processing systems*, 33:21271–21284, 2020.
- [20] Ziyu Guo, Renrui Zhang, Longtian Qiu, Xianzheng Ma, Xupeng Miao, Xuming He, and Bin Cui. Calip: Zero-shot enhancement of clip with parameter-free attention. In *Proceedings of the AAAI Conference on Artificial Intelligence*, volume 37, pages 746–754, 2023.
- [21] Kaiming He, Haoqi Fan, Yuxin Wu, Saining Xie, and Ross Girshick. Momentum contrast for unsupervised visual representation learning. In *Proceedings of the IEEE/CVF conference on computer vision and pattern recognition*, pages 9729–9738, 2020.
- [22] Kaiming He, Xiangyu Zhang, Shaoqing Ren, and Jian Sun. Deep residual learning for image recognition. In *Proceedings of the IEEE conference on computer vision and pattern recognition*, pages 770–778, 2016.
- [23] Ruifei He, Shuyang Sun, Xin Yu, Chuhui Xue, Wenqing Zhang, Philip Torr, Song Bai, and XIAOJUAN QI. Is synthetic data from generative models ready for image recognition? In *The Eleventh International Conference on Learning Representations*, 2022.
- [24] Patrick Helber, Benjamin Bischke, Andreas Dengel, and Damian Borth. Eurosat: A novel dataset and deep learning benchmark for land use and land cover classification. *IEEE Journal of Selected Topics in Applied Earth Observations and Remote Sensing*, 12(7):2217–2226, 2019.
- [25] Martin Heusel, Hubert Ramsauer, Thomas Unterthiner, Bernhard Nessler, and Sepp Hochreiter. Gans trained by a two time-scale update rule converge to a local nash equilibrium. *Advances in neural information processing systems*, 30, 2017.
- [26] Chao Jia, Yinfei Yang, Ye Xia, Yi-Ting Chen, Zarana Parekh, Hieu Pham, Quoc Le, Yun-Hsuan Sung, Zhen Li, and Tom Duerig. Scaling up visual and vision-language representation learning with noisy text supervision. In *International conference on machine learning*, pages 4904–4916. PMLR, 2021.
- [27] Chao Jia, Yinfei Yang, Ye Xia, Yi-Ting Chen, Zarana Parekh, Hieu Pham, Quoc Le, Yun-Hsuan Sung, Zhen Li, and Tom Duerig. Scaling up visual and vision-language representation learning with noisy text supervision. In *International conference on machine learning*, pages 4904–4916. PMLR, 2021.
- [28] Tosio Kato. *Perturbation theory for linear operators*, volume 132. Springer Science & Business Media, 2013.
- [29] Jonathan Krause, Michael Stark, Jia Deng, and Li Fei-Fei. 3d object representations for fine-grained categorization. In *Proceedings of the IEEE international conference on computer vision workshops*, pages 554–561, 2013.
- [30] Ananya Kumar, Aditi Raghunathan, Robbie Jones, Tengyu Ma, and Percy Liang. Fine-tuning can distort pretrained features and underperform out-of-distribution. *arXiv preprint arXiv:2202.10054*, 2022.
- [31] Ilya Loshchilov and Frank Hutter. Decoupled weight decay regularization. In *International Conference on Learning Representations*, 2019.
- [32] Subhransu Maji, Esa Rahtu, Juho Kannala, Matthew Blaschko, and Andrea Vedaldi. Fine-grained visual classification of aircraft. *arXiv preprint arXiv:1306.5151*, 2013.
- [33] Sachit Menon and Carl Vondrick. Visual classification via description from large language models. In *The Eleventh International Conference on Learning Representations*, 2023.
- [34] Alexander Quinn Nichol, Prafulla Dhariwal, Aditya Ramesh, Pranav Shyam, Pamela Mishkin, Bob McGrew, Ilya Sutskever, and Mark Chen. Glide: Towards photorealistic image generation and editing with text-guided diffusion models. In *International Conference on Machine Learning*, pages 16784–16804. PMLR, 2022.
- [35] Maria-Elena Nilsback and Andrew Zisserman. Automated flower classification over a large number of classes. In *2008 Sixth Indian conference on computer vision, graphics & image processing*, pages 722–729. IEEE, 2008.
- [36] Maxime Oquab, Timothée Darcet, Théo Moutakanni, Huy Vo, Marc Szafraniec, Vasil Khalidov, Pierre Fernandez, Daniel Haziza, Francisco Massa, Alaaeldin El-Nouby, et al. Dinov2: Learning robust visual features without supervision. *arXiv preprint arXiv:2304.07193*, 2023.

- [37] Omkar M Parkhi, Andrea Vedaldi, Andrew Zisserman, and CV Jawahar. Cats and dogs. In *2012 IEEE conference on computer vision and pattern recognition*, pages 3498–3505. IEEE, 2012.
- [38] Hieu Pham, Zihang Dai, Golnaz Ghiasi, Kenji Kawaguchi, Hanxiao Liu, Adams Wei Yu, Jiahui Yu, Yi-Ting Chen, Minh-Thang Luong, Yonghui Wu, et al. Combined scaling for zero-shot transfer learning. *Neurocomputing*, 555:126658, 2023.
- [39] Dustin Podell, Zion English, Kyle Lacey, Andreas Blattmann, Tim Dockhorn, Jonas Müller, Joe Penna, and Robin Rombach. Sdxl: Improving latent diffusion models for high-resolution image synthesis. *arXiv preprint arXiv:2307.01952*, 2023.
- [40] Sarah Pratt, Ian Covert, Rosanne Liu, and Ali Farhadi. What does a platypus look like? generating customized prompts for zero-shot image classification. In *Proceedings of the IEEE/CVF International Conference on Computer Vision*, pages 15691–15701, 2023.
- [41] Alec Radford, Jong Wook Kim, Chris Hallacy, Aditya Ramesh, Gabriel Goh, Sandhini Agarwal, Girish Sastry, Amanda Askell, Pamela Mishkin, Jack Clark, et al. Learning transferable visual models from natural language supervision. In *International conference on machine learning*, pages 8748–8763. PMLR, 2021.
- [42] Aditya Ramesh, Mikhail Pavlov, Gabriel Goh, Scott Gray, Chelsea Voss, Alec Radford, Mark Chen, and Ilya Sutskever. Zero-shot text-to-image generation. In *International Conference on Machine Learning*, pages 8821–8831. PMLR, 2021.
- [43] Robin Rombach, Andreas Blattmann, Dominik Lorenz, Patrick Esser, and Björn Ommer. High-resolution image synthesis with latent diffusion models. In *Proceedings of the IEEE/CVF conference on computer vision and pattern recognition*, pages 10684–10695, 2022.
- [44] Chitwan Saharia, William Chan, Saurabh Saxena, Lala Li, Jay Whang, Emily L Denton, Kamyar Ghasemipour, Raphael Gontijo Lopes, Burcu Karagol Ayan, Tim Salimans, et al. Photorealistic text-to-image diffusion models with deep language understanding. *Advances in Neural Information Processing Systems*, 35:36479–36494, 2022.
- [45] Mert Bulent Sariyildiz, Karteek Alahari, Diane Larlus, and Yannis Kalantidis. Fake it till you make it: Learning transferable representations from synthetic imagenet clones. In *CVPR 2023—IEEE/CVF Conference on Computer Vision and Pattern Recognition*, 2023.
- [46] Khurram Soomro, Amir Roshan Zamir, and Mubarak Shah. Ucf101: A dataset of 101 human actions classes from videos in the wild. *arXiv preprint arXiv:1212.0402*, 2012.
- [47] Gilbert Strang. *Introduction to linear algebra*. SIAM, 2022.
- [48] Yonglong Tian, Lijie Fan, Phillip Isola, Huiwen Chang, and Dilip Krishnan. Stablerep: Synthetic images from text-to-image models make strong visual representation learners. *arXiv preprint arXiv:2306.00984*, 2023.
- [49] Vishaal Udandarao, Ankush Gupta, and Samuel Albanie. Sus-x: Training-free name-only transfer of vision-language models. In *Proceedings of the IEEE/CVF International Conference on Computer Vision*, pages 2725–2736, 2023.
- [50] Mitchell Wortsman, Gabriel Ilharco, Jong Wook Kim, Mike Li, Simon Kornblith, Rebecca Roelofs, Raphael Gontijo Lopes, Hannaneh Hajishirzi, Ali Farhadi, Hongseok Namkoong, et al. Robust fine-tuning of zero-shot models. In *Proceedings of the IEEE/CVF Conference on Computer Vision and Pattern Recognition*, pages 7959–7971, 2022.
- [51] Jianxiong Xiao, James Hays, Krista A Ehinger, Aude Oliva, and Antonio Torralba. Sun database: Large-scale scene recognition from abbey to zoo. In *2010 IEEE computer society conference on computer vision and pattern recognition*, pages 3485–3492. IEEE, 2010.
- [52] Jure Zbontar, Li Jing, Ishan Misra, Yann LeCun, and Stéphane Deny. Barlow twins: Self-supervised learning via redundancy reduction. In *International Conference on Machine Learning*, pages 12310–12320. PMLR, 2021.
- [53] Renrui Zhang, Xiangfei Hu, Bohao Li, Siyuan Huang, Hanqiu Deng, Yu Qiao, Peng Gao, and Hongsheng Li. Prompt, generate, then cache: Cascade of foundation models makes strong few-shot learners. In *Proceedings of the IEEE/CVF Conference on Computer Vision and Pattern Recognition*, pages 15211–15222, 2023.

- [54] Renrui Zhang, Wei Zhang, Rongyao Fang, Peng Gao, Kunchang Li, Jifeng Dai, Yu Qiao, and Hongsheng Li. Tip-adapter: Training-free adaption of clip for few-shot classification. In *European Conference on Computer Vision*, pages 493–510. Springer, 2022.
- [55] Kaiyang Zhou, Jingkang Yang, Chen Change Loy, and Ziwei Liu. Learning to prompt for vision-language models. *International Journal of Computer Vision (IJCV)*, 2022.
- [56] Jiachen Zhu, Ravid Shwartz-Ziv, Yubei Chen, and Yann LeCun. Variance-covariance regularization improves representation learning. *arXiv preprint arXiv:2306.13292*, 2023.

Appendix / supplemental material

A Additional details for the name-only transfer experiments

Additional implementation details We fine-tuned the classifier with the generated dataset for 10 epochs. The learning rate was set to 3×10^{-5} with a cosine schedule and 500 warm-up steps. A batch size was set to 128, and the optimizer employed was AdamW [31]. The weight mixing coefficient α is searched in intervals of 0.1 from 0 to 1, and λ_{var} , λ_{cov} are searched on $\{0.08, 0.16, 0.32, 0.64, 1.28\}$, $\{0.01, 0.02, 0.04, 0.08, 0.16\}$, respectively. In our experiments, for generating 64 images for 1000 classes to construct the ImageNet dataset, it takes 2 days with 4 RTX 3090. Then, fine-tuning the classifier with the generated ImageNet dataset takes 2 hours with a single RTX 3090. The other datasets are in proportion to the number of the classes. The entire training and test code will be made publicly available.

Licenses for existing assets For the datasets, we have checked that ImageNet (Custom (research, non-commercial)) [12]², Caltech101 [15] (CC-BY 4.0)³, DTD [10] (Custom (research-only))⁴, EuroSAT [24] (MIT)⁵, FGVCAircraft [32] (Custom (non-commercial))⁶, OxfordPets [37] (CC BY-SA 4.0)⁷, and StanfordCars [29] (Custom (non-commercial))⁸ can be used for research purposes, but Flowers102 [35]⁹, Food101 [4]¹⁰, SUN397 [51]¹¹, and UCF101 [46]¹² do not exist the license or term of use information online. Thus, we reached out to the authors, and we are waiting for their responses. For the pre-trained models, we have checked that DALL-E [42] (Custom)¹³, DALL-E mini [11] (Custom)¹⁴, Stable Diffusion [43] (Creative ML OpenRAIL-M)¹⁵, Stable Diffusion XL [39] (Creative ML OpenRAIL-M)¹⁶, and CLIP [41] (MIT)¹⁷ can be used for research purposes.

Experiments on Various CLIP Architectures While the CLIP ViT-B/16 [13, 41] has demonstrated high performance in the name-only transfer, it is important to note that the effectiveness of our proposed approach extends beyond this specific model architecture. In the main paper, we consistently use the CLIP ViT-B/16 image encoder for all experiments. In this section, we aim to illustrate that our approach is versatile across various CLIP architectures, including ResNet-50 [22], ResNet-101 [22], and ViT-B/32 [13], as detailed in Table 4.

Our experiments reveal notable improvements with the proposed approach, particularly on ViT-based image encoders, which consistently outperform the name-only transfer baselines. Additionally, our results indicate generally superior performance on the 11 datasets when utilizing ResNet-based image encoders. This finding underscores the applicability of our method across diverse CLIP architectures.

B Detailed Ablation Studies Across 11 Datasets

The ablation studies of the proposed method in the name-only transfer scenario are conducted across all 11 datasets as illustrated in Table 5. The generated datasets are synthesized by Stable Diffusion

²<https://image-net.org/>

³<https://data.caltech.edu/records/mzrjq-6wc02>

⁴<https://www.robots.ox.ac.uk/~vgg/data/dtd/>

⁵<https://github.com/phelber/eurosat>

⁶<https://www.robots.ox.ac.uk/~vgg/data/fgvc-aircraft>

⁷<https://www.robots.ox.ac.uk/~vgg/data/pets/>

⁸https://ai.stanford.edu/~jkrause/cars/car_dataset.html

⁹<https://www.robots.ox.ac.uk/~vgg/data/flowers/102/index.html>

¹⁰https://data.vision.ee.ethz.ch/cvl/datasets_extra/food-101/

¹¹<https://vision.princeton.edu/projects/2010/SUN/>

¹²<https://www.crcv.ucf.edu/data/UCF101.php>

¹³<https://openai.com/policies/terms-of-use/>

¹⁴<https://www.craiyon.com/terms>

¹⁵<https://stablediffusion.gitbook.io/overview/stable-diffusion-overview/license>

¹⁶https://github.com/Stability-AI/generative-models/blob/main/model_licenses/LICENSE-SDXL1.0

¹⁷<https://github.com/openai/CLIP/blob/main/LICENSE>

Table 4: Comparison of accuracy on 11 name-only transfer benchmarks with ResNet-50, ResNet-101 [22], and ViT-B/32 [13] CLIP image encoder [41]. Average indicates the average accuracy on 11 datasets. Underline represents the highest accuracy achieved when utilizing generated datasets by DALL-E [42] given by CaFo [53], while **Bold** indicates the highest accuracy achieved without any constraints.

ResNet-50	Average	ImageNet	Caltech101	DTD	EuroSAT	FGVC	Flowers102	Food101	OxfordPets	StanfordCars	SUN397	UCF101
ZS CLIP	56.28	60.20	85.15	41.84	28.80	16.95	61.39	73.22	81.77	55.74	58.58	55.46
CALIP	56.56	60.35	88.48	40.79	26.11	16.24	63.12	74.13	81.96	56.30	59.18	55.46
CuPL	60.82	61.62	88.28	50.12	37.48	20.70	77.64	64.31	86.43	57.06	62.25	63.18
SuS-X (DALL-E)	61.05	61.93	89.41	47.64	38.91	19.95	<u>66.99</u>	77.64	86.35	56.66	62.71	63.39
CaFo (DALL-E)	61.84	62.48	<u>90.83</u>	49.47	42.65	20.58	65.94	77.54	86.45	58.66	62.68	62.94
Ours (DALL-E)	<u>62.18</u>	<u>62.39</u>	91.20	<u>50.83</u>	41.64	20.34	<u>66.99</u>	77.56	<u>87.22</u>	<u>60.19</u>	<u>63.06</u>	62.57
CaFo (SDv2.1)	61.30	62.16	89.74	49.88	37.49	20.64	63.91	77.62	87.00	59.71	62.77	63.39
CaFo (SDXL)	61.26	61.46	88.32	49.76	38.41	20.82	64.96	77.53	87.05	60.12	62.08	63.36
Ours (SDv2.1)	63.05	62.76	90.87	51.95	48.14	20.10	66.22	77.56	87.05	62.58	63.23	63.10
Ours (SDXL)	62.97	62.67	91.08	50.18	45.40	20.10	66.99	77.56	87.41	64.53	62.87	63.89
ResNet-101	Average	ImageNet	Caltech101	DTD	EuroSAT	FGVC	Flowers102	Food101	OxfordPets	StanfordCars	SUN397	UCF101
ZS CLIP	58.58	62.20	89.33	42.38	30.07	18.00	61.84	77.38	83.65	62.74	59.38	57.39
CALIP	58.17	62.33	90.47	41.67	24.04	17.16	62.04	77.67	83.70	62.73	59.94	58.13
CuPL	59.91	60.44	90.18	48.82	28.36	18.60	61.71	80.09	85.88	60.60	61.58	62.70
SuS-X (DALL-E)	61.87	62.42	91.89	48.17	41.51	18.87	65.49	80.49	85.04	61.55	62.51	62.68
CaFo (DALL-E)	62.81	63.83	93.27	49.23	46.04	18.87	62.89	<u>80.23</u>	87.30	63.35	62.51	63.42
Ours (DALL-E)	64.09	<u>64.09</u>	<u>93.35</u>	52.36	48.68	<u>20.79</u>	65.61	80.46	<u>87.98</u>	<u>65.09</u>	<u>63.10</u>	<u>63.44</u>
CaFo (SDv2.1)	61.90	63.07	91.72	49.94	34.40	19.56	62.28	80.34	87.76	66.22	62.77	62.78
CaFo (SDXL)	61.00	61.80	90.79	49.17	30.21	19.26	61.75	80.15	87.38	64.73	61.97	63.73
Ours (SDv2.1)	63.91	64.52	93.59	50.71	45.49	19.92	64.88	80.28	89.32	67.57	63.39	63.36
Ours (SDXL)	64.09	64.15	93.43	51.48	42.26	22.17	65.29	80.35	89.32	69.87	62.83	63.89
ViT-B/32	Average	ImageNet	Caltech101	DTD	EuroSAT	FGVC	Flowers102	Food101	OxfordPets	StanfordCars	SUN397	UCF101
ZS CLIP	60.61	64.10	91.76	43.38	42.17	18.84	63.78	78.35	80.49	60.33	62.19	61.35
CALIP	60.93	63.82	92.78	43.26	43.98	18.51	64.07	78.91	81.06	60.10	62.83	60.96
CuPL	64.12	64.92	92.21	49.76	47.70	21.78	67.28	80.84	89.10	60.83	65.40	65.56
SuS-X (DALL-E)	64.56	65.14	93.35	47.87	51.26	21.06	69.22	80.78	89.07	61.15	65.68	65.58
CaFo (DALL-E)	65.13	65.52	93.79	50.83	52.86	22.38	67.68	80.88	89.07	61.82	65.87	65.74
Ours (DALL-E)	65.75	<u>65.63</u>	<u>93.63</u>	<u>52.48</u>	<u>52.41</u>	22.53	<u>70.16</u>	80.90	<u>89.94</u>	<u>62.77</u>	<u>66.49</u>	<u>66.32</u>
CaFo (SDv2.1)	64.54	65.18	93.18	50.24	47.80	22.11	66.91	80.81	89.53	62.67	65.96	65.50
CaFo (SDXL)	64.69	64.69	92.70	50.30	49.78	21.78	67.60	80.67	90.11	62.73	65.26	66.01
Ours (SDv2.1)	66.50	66.08	94.12	54.85	54.16	22.35	68.90	80.69	90.30	65.85	66.97	67.22
Ours (SDXL)	66.74	66.03	94.04	52.48	54.78	22.50	70.85	80.69	90.16	69.34	66.06	67.25

Table 5: Ablation studies of the weight-space ensemble and variance-covariance regularization across all 11 datasets. It shows the general improvements of the proposed method for all datasets.

Fine-tune Classifier	Weight-space Ensemble	\mathcal{L}_{VCR}	Average	ImageNet	Caltech101	DTD	EuroSAT	FGVC
\times	\times	\times	67.12	69.65	94.28	54.55	40.70	27.90
\checkmark	\times	\times	53.79	50.18	77.57	49.00	50.96	12.75
\checkmark	\checkmark	\times	69.13	70.51	94.28	57.74	50.96	27.90
\checkmark	\checkmark	\checkmark	69.56	70.79	94.93	57.98	50.99	27.90
Fine-tune Classifier	Weight-space Ensemble	\mathcal{L}_{VCR}	Flowers102	Food101	OxfordPets	StanfordCars	SUN397	UCF101
\times	\times	\times	69.47	86.35	90.54	66.62	68.00	70.29
\checkmark	\times	\times	43.93	51.60	86.32	62.89	55.31	51.18
\checkmark	\checkmark	\times	70.36	86.35	91.66	70.77	69.40	70.45
\checkmark	\checkmark	\checkmark	71.38	86.35	92.31	71.68	69.84	70.87

Few-shot Classification Results on 11 datasets

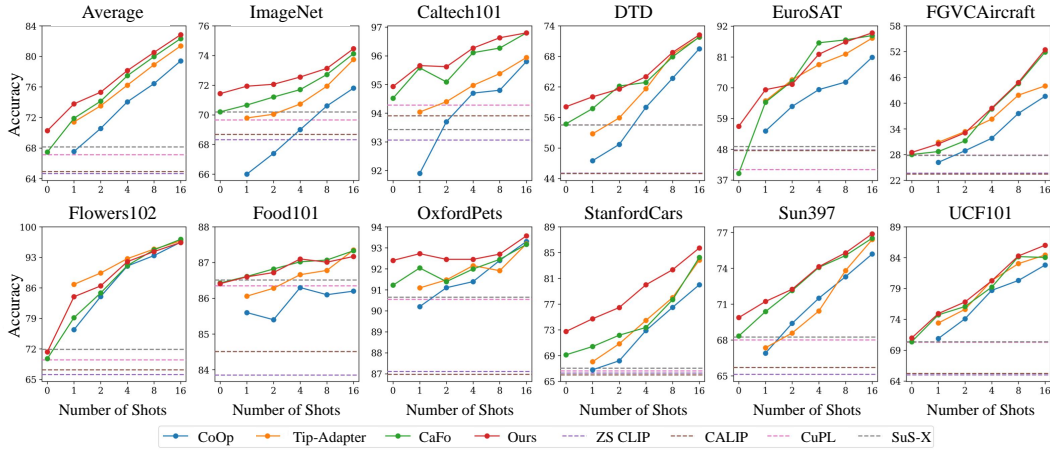


Figure 8: Comparison of accuracy in the few-shot classification setting for all 11 datasets. Although the enhanced CLIP image encoder has been fine-tuned on the name-only transfer scenario, the experiments show its versatility across various datasets.

2.1 [43]. Our comprehensive experiments consistently demonstrate the efficacy of the training-time and post-training regularization techniques. The post-training regularization, weight-space ensemble, successfully overcame the performance degradation of fine-tuning the entire classifier by leveraging the zero-shot classifier. While the weight-space ensemble does not require any additional computational cost, it shows significant and consistent improvements across all datasets. Furthermore, the training-time regularization (\mathcal{L}_{VCR}) generally shows superior performance across all datasets except two datasets by incorporating the weight-space ensemble.

C Detailed Results on Few-shot Classification

In Figure 8, we present the few-shot classification results across all 11 datasets. Our experiments employ CuPL [40] text prompts and the CaFo [53] adapter to achieve these outcomes. We compare the proposed method with the adaptation of the vision-language approaches for few-shot classification: CoOp [55], Tip-Adapter [54], and CaFo [53]. Additionally, the experiment incorporates name-only transfer approaches, depicted as a dotted line, following methods like CLIP [41], CALIP [20], CuPL [40], and SuS-X [49]. The results show the effectiveness of our proposed approach in few-shot classification, even when constrained to training solely on generated datasets.

D Impact of Text-to-image Generation Models

By scaling up the training datasets for text-to-image generation models, they can produce high-fidelity and diverse images from textual input. Although every recent generative model effectively incorporates the textual condition, there is a noticeable difference between generative models in the diversity of the generated images. While DALL-E [42] tends to generate more canonical and traditional images for each class, SDv2.1 [43] and SDXL [39] exhibit a wider range of styles from the same textual condition, as depicted in Figure 9.

The diversity of the generated images plays a crucial role in the name-only transfer, especially when the learnable parameters are insufficient. Previous approaches in the name-only transfer often resorted to overcoming the domain gap between real and generated images by reducing the number of learnable parameters. Consequently, they were unable to leverage diverse generated datasets due to their limited capacity. In contrast, we successfully fine-tuned the entire classifier by implementing the proposed regularization techniques. As a result, the disparity in average accuracy between CaFo [53] and Ours increases when employing different text-to-image generation models, as depicted in Figure 10.

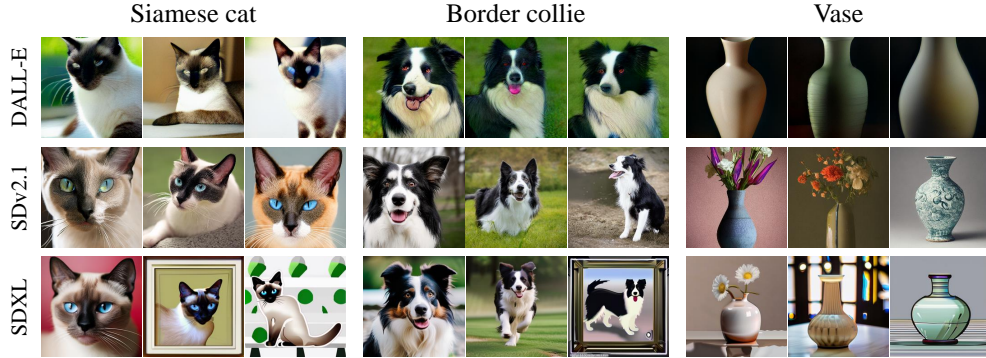


Figure 9: Qualitative results for the various text-to-image generation models. While DALL-E generates conventional images, SDv2.1 and SDXL generate in various styles.

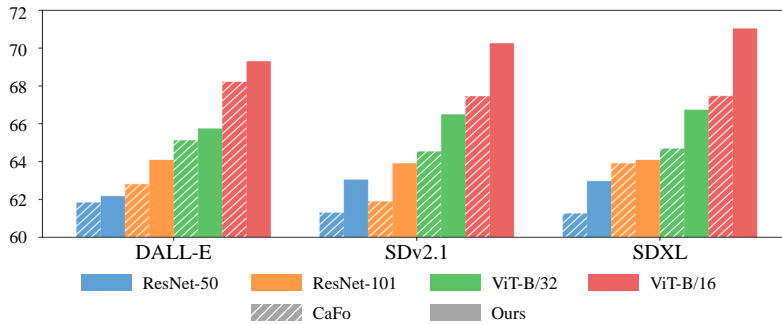


Figure 10: The average accuracy of the name-only transfer experiments across 11 datasets with various CLIP backbones by changing the text-to-image generation models. The performance gaps between CaFo and Ours increase according to the generation models.

E Mixing Coefficient of the Weight-space Ensemble for Each Dataset

The mixing coefficient α of the weight-space ensemble, a crucial hyper-parameter in our proposed approach, plays a pivotal role in achieving optimal results. Through experiments across 11 datasets, we found that a fixed mixing coefficient α of 0.2 consistently yields substantial performance gains from the generated datasets. However, we recognize the need to tailor mixing coefficients individually for each dataset, considering the varying domain gaps between real and generated datasets, as illustrated in Table 6. For example, the EuroSAT dataset [24] demands a mixing coefficient α of 1.0 due to the remarkable realism exhibited by the generated EuroSAT dataset, as depicted in Figure 12.

As discussed in the limitations of the main paper, the weight-space ensemble, involving fine-tuned models trained on generated datasets, does not outperform the zero-shot classifier in specific domains such as FGVC Aircraft [32] and Food101 [4] due to challenges in generation quality for fine-grained classification. Despite these limitations in fine-grained classification datasets, our experiments highlight the effectiveness of the weight-space ensemble, particularly in the name-only transfer of vision-language models, as depicted in Table 6.

F Compatibility with other name-only transfer approaches

The challenge of a persistent domain gap between real and generated datasets remains a significant hurdle in the name-only transfer scenario. As a result, previous approaches in the name-only transfer scenario have predominantly focused on enriching prompts [40] with large-language models [5] and adapters [49, 53] to avoid training the numerous parameters within the CLIP image encoder. In contrast, we successfully enhanced the CLIP image encoder by utilizing a weight-space ensemble and variance-covariance regularization on the generated image features in the name-only transfer

Table 6: Accuracy on each dataset by changing the mixing coefficient α . The experiments have been conducted on the final model that employs the enriched prompts [40] and the training-time regularization (\mathcal{L}_{VCR}).

α	0.0	0.1	0.2	0.3	0.4	0.5	0.6	0.7	0.8	0.9	1.0
ImageNet	69.65	70.79	70.48	69.34	67.73	65.46	62.90	59.97	56.53	52.66	48.38
Caltech101	94.28	94.93	94.77	94.44	94.20	93.75	92.86	91.52	90.26	88.15	85.19
DTD	54.55	56.44	57.62	57.92	57.98	57.86	56.50	54.96	53.72	52.07	50.35
EuroSAT	40.70	42.81	44.72	46.54	48.04	48.95	49.44	49.91	50.37	50.83	50.99
FGVC	27.90	27.00	26.34	25.11	23.01	21.66	20.01	18.39	17.01	15.66	14.73
Flowers102	69.47	70.73	71.38	70.48	69.22	66.18	63.05	60.01	55.38	51.04	47.71
Food101	86.35	85.91	84.72	82.62	79.87	76.34	72.20	67.47	62.50	57.29	51.90
OxfordPets	90.54	91.36	91.80	92.07	92.31	91.99	91.71	91.01	90.22	89.15	88.09
StanfordCars	66.62	69.21	70.64	71.45	71.68	71.17	70.63	69.34	67.98	65.73	63.31
SUN397	68.00	69.36	69.84	69.45	68.14	66.49	64.44	62.30	59.83	57.17	54.26
UCF101	70.29	70.87	70.87	70.26	68.94	67.14	64.37	61.93	58.68	55.38	52.50
Average	67.12	68.13	68.47	68.15	67.38	66.09	64.37	62.44	60.23	57.74	55.22

Table 7: Results obtained from the integration of our regularized fine-tuning method with other name-only transfer approaches by leveraging Stable Diffusion 2.1 [43]. The blue subscripts indicate the performance improvements from the zero-shot CLIP.

Regularized Fine-tuning	Enriching Prompts [40]	Adapter [53]	Average Accuracy
\times	\times	\times	64.66
\checkmark	\times	\times	67.66 (+3.00)
\checkmark	\checkmark	\times	69.55 (+4.89)
\checkmark	\checkmark	\checkmark	70.26 (+5.60)

scenario. Departing from existing approaches, our objective of improving classification performance follows a unique path. We showcase the performance gains of our name-only transfer method along with enriching prompts from CuPL [40] and adapter from CaFo [53] in Table 7. In summary, our aim is to unlock the image encoder’s substantial potential and showcase its compatibility with other name-only transfer approaches, ultimately enabling ours to outperform existing methods successfully.

G Hand-written Prompts to Synthesize Images

The prompt engineering for text-to-image generation models is one of the crucial engineering techniques for synthesizing high-quality images. While “a photo of a [class name]” serves as a general and potent prompt for producing high-quality images, its effectiveness is notably constrained when in fine-grained classifications, *e.g.*, EuroSAT [24] and FGVC Aircraft [32]. Therefore, we adopt the standard hand-written text prompt from CLIP followed by prior research [23, 49, 53].

We demonstrate the impact of the hand-written prompts in the synthesis of EuroSAT images. Although the images generated by utilizing both prompts are realistic and appropriately convey the target class, the images generated from “a photo of a forest.” are totally different from the original EuroSAT images as shown in Figure 11. Therefore, we utilize the hand-written prompts for generating datasets given by previous approaches [23, 49, 53]. The specific hand-written prompts used for the evaluation of 11 datasets can be found in Table 8, and the generated images for these 11 datasets are showcased in Figures 12 and 13.

Given the pivotal role that manual prompt engineering plays in generating datasets, exploring automatic prompt engineering techniques emerges as a crucial avenue for future research.

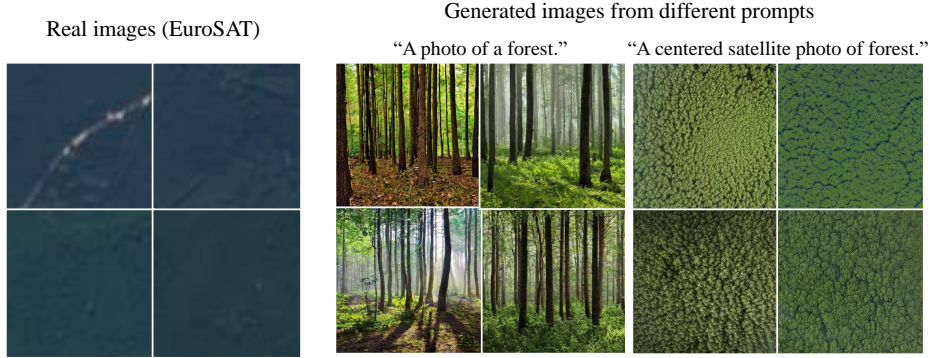


Figure 11: The generated images from two different prompts: “a photo of a forest.” and “a centered satellite photo of a forest.”. Since the EuroSAT is the satellite domain dataset, the general prompts are limited to reducing the domain gap between the real and generated images with minimal effort.

Table 8: Hand-written prompts used for generating images given by previous researches [23, 49, 53]. These hand-written text prompts are selected from the standard text prompts for zero-shot classification with CLIP.

Dataset	Hand-written Prompts
ImageNet	a photo of a [class name].
Caltech101	a photo of a [class name].
DTD	a photo of a [class name] texture.
EuroSAT	a centered satellite photo of [class name].
FGVC	a photo of a [class name], a type of aircraft.
Food101	a photo of [class name], a type of food.
Flowers102	a photo of a [class name], a type of flower.
OxfordPets	a photo of a [class name], a type of pet.
StanfordCars	a photo of a [class name], a type of car.
SUN397	a photo of a [class name].
UCF101	a photo of a person doing [class name].

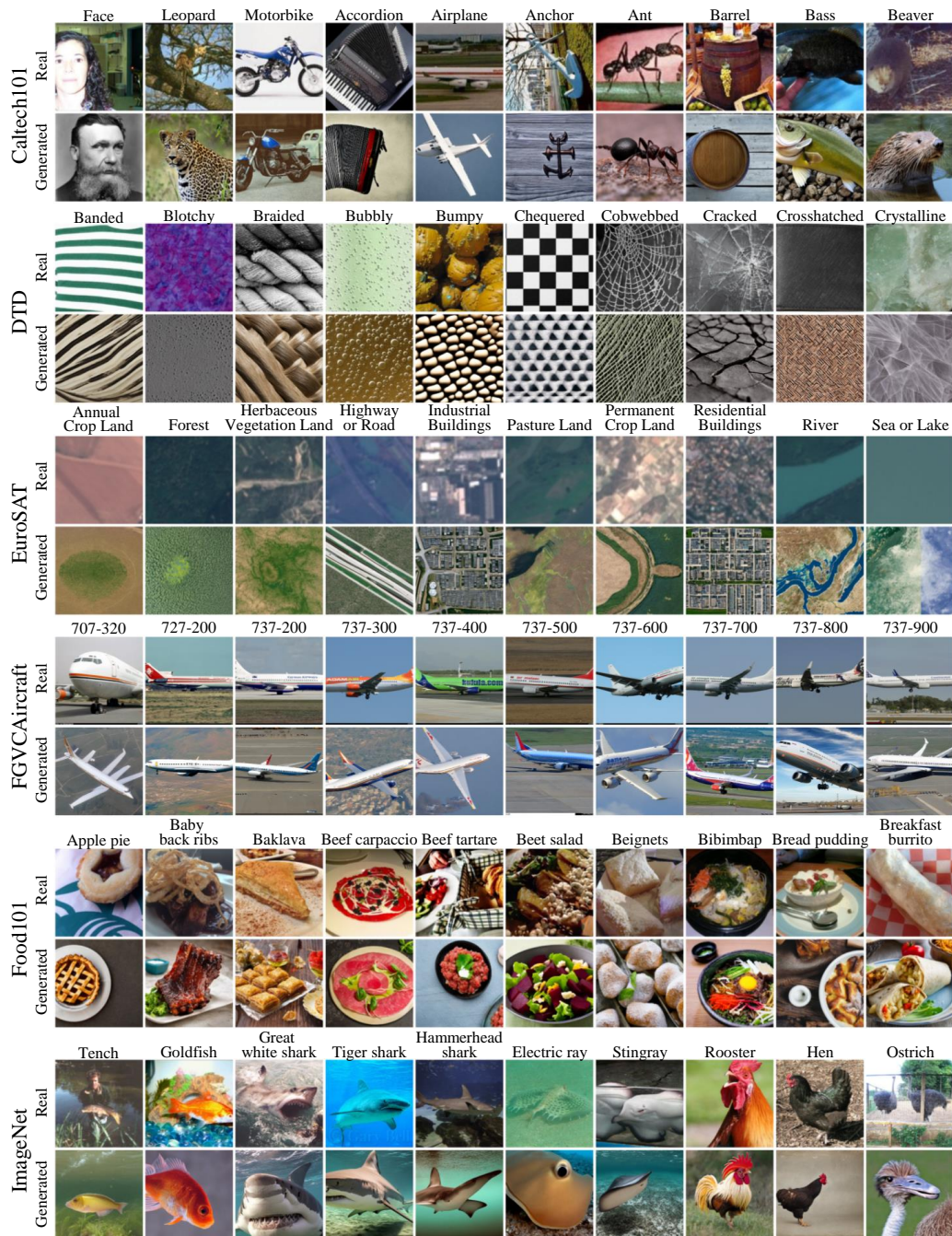


Figure 12: Qualitative results of the generated datasets. The first row contains the real images, and the second row contains the generated images for each dataset.

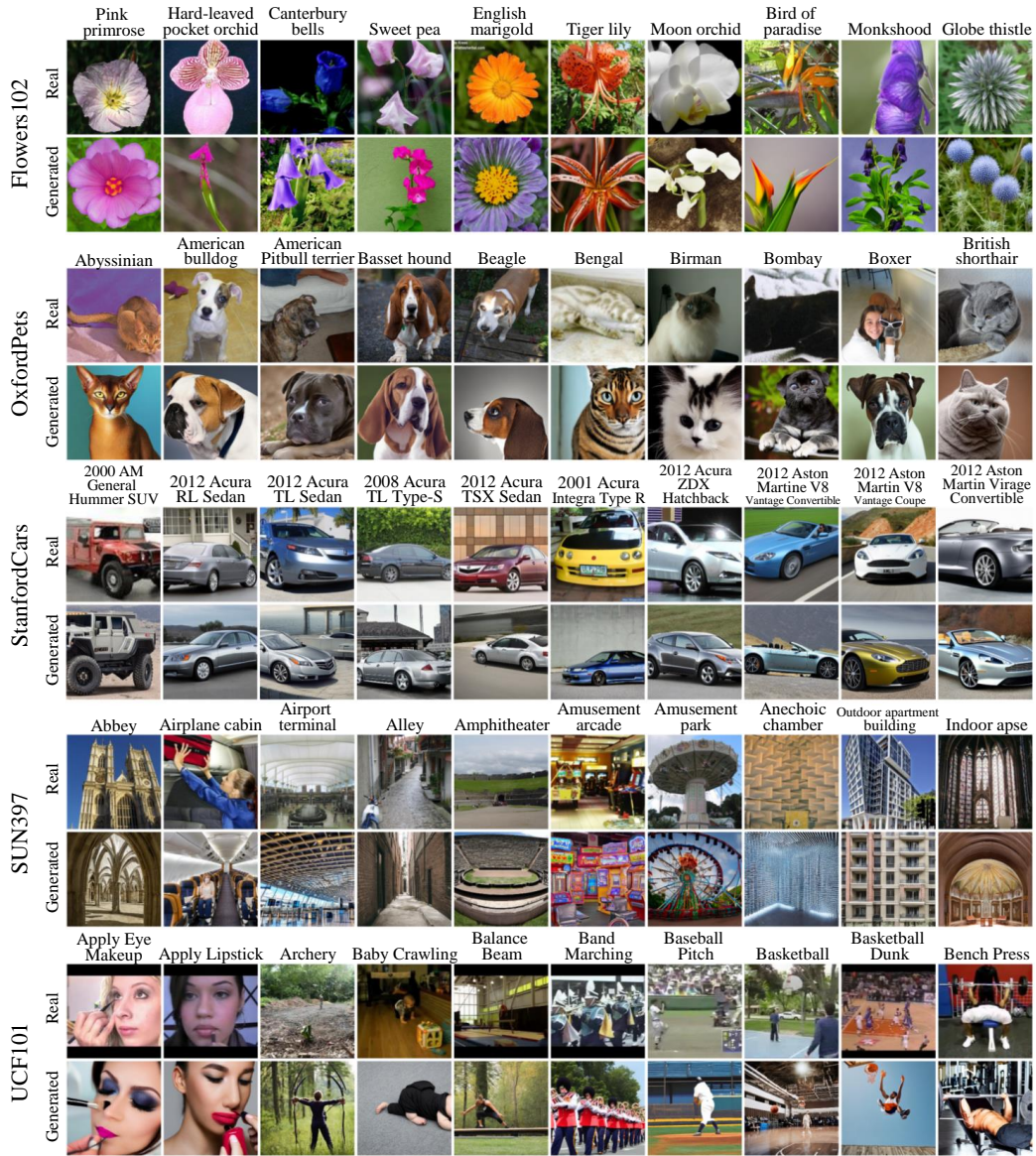


Figure 13: Qualitative results of the generated datasets. The first row contains the real images, and the second row contains the generated images for each dataset.